

High-performance high dynamic range image generation by inverted local patterns

ISSN 1751-9659


Received on 14th February 2014

Revised on 28th May 2015

Accepted on 22nd June 2015

doi: 10.1049/iet-ipr.2014.0853

www.ietdl.org

Shih-Chang Hsia , Ting-Tseng Kuo

Department of Electronics Engineering, National Yunlin University of Science and Technology, Douliou, Yunlin, Taiwan

✉ E-mail: hsia@yuntech.edu.tw

Abstract: This study presents an image processing algorithm capable of generating high dynamic range (HDR) images from a single frame. On the basis of liquid crystal display (LCD) backlight theory, the proposed algorithm uses an inverted local pattern approach to adjust the histogram of lighting distribution. To improve processing efficiency, sampled images are classified into three types according to exposure characteristics, which are used to obtain suitable processing factor. The inverting factor is mixed with the original sample to darken the bright areas and brighten the dark areas in the images. Brightness enhancement and auto-gain control are then added to expand the range of the grey levels. Authors' results demonstrate the efficacy of the proposed HDR algorithm in improving shadow details. In addition, single-pass processing is used to reduce computational complexity, making the algorithm applicable for low-power portable cameras and video recorders.

1 Introduction

Cameras are widely used to record video signals; however, variations in environmental lighting mean that exposure times must be adjusted according to ambient conditions. In bright sunlight, exposure times must be shortened to avoid positive saturation. Conversely, when the camera is operated in dark conditions, the exposure time must be extended to avoid negative saturation. However, when an image contains both bright and dark areas, positive and negative saturation exists within the same frame. This tends to degrade the visual quality due to the fact that the details cannot be rendered accurately in the excessively dark and bright areas.

High dynamic range (HDR) algorithms have been developed to deal with this problem by expanding the dynamic range of the images, that is, by expanding the range in which details can be rendered in both the bright and dark areas in a single frame. HDR digital photography was first developed nearly two decades ago, a variation first developed by Mann [1]. Multiple exposure methods [2–5] are commonly used to expand the dynamic range. Three images obtained using three different exposures can be merged using gradient-based synthesis [4]. Pixels in the HDR image are computed by comparing the three images according to Gaussian blending and cutting functions with the aim of preserving the highest quality portions from each of the three images, which are then combined to form a single HDR image. Unfortunately, the multiple exposure approach requires long processing time and high computational costs. To reduce this, Vonikakis *et al.* [6] recently proposed a single exposure algorithm comprising three stages: linear stretching, block parameter estimation, and contrast modification. This approach is able to rapidly produce HDR images; however, the down- and up-sample may degrade image resolution. Guarnieri *et al.* [7] used logarithms and exponential-based edge-preserving low-pass and multi-resolution acceleration. Unfortunately, the use of iterative operations inevitably increases computation time. Kim *et al.* [8] presented a retinex algorithm with a tone mapping function to improve the contrast in dark areas; however, these methods are ineffective when seeking to reduce positive saturation in over-exposed regions [7–9]. In [10], eight graphic processing units were used in conjunction with the Pattanaik operator for tone mapping in real time. Similar to HDR algorithms based on histogram equalisation [11, 12], this method is able to smooth histogram distribution in

order to balance the light; however, the processed image can appear unnatural in areas where artefacts occur.

In this study, we developed a high-performance HDR algorithm that uses only a single-image and one-pass processing flow (as opposed to an iterative approach) to accelerate computation. On the basis of LCD backlight theory, we propose an inverted pattern approach to improve over- and under-exposed regions within the same frame. The remainder of this paper is organised as follows. We present the proposed HDR algorithm in Section 2. A practical implementation and experiments are outlined in Section 3. Comparisons with the existing methods are presented in Section 4 and conclusions are drawn in Section 5.

2 Proposed fast algorithm for HDR image generation

The proposed HDR algorithm is based on a theory similar to that used in local dimming for LCD backlights [13]. In the local dimming of LCDs, illumination from the backlight corresponds to block image brightness. Illumination is increased for bright blocks and reduced for dark blocks. We used this concept in the development of an HDR algorithm using inverted local patterns. The factor of inverted local patterns is computed from the original sampled pixels. In the event that the sampling level is too low, then the inversion factor is increased. The level of dark regions can be enhanced when backlighting is increased, and highlights can be preserved by reducing backlighting to produce HDR images.

Fig. 1 presents a flowchart of the proposed HDR algorithm. First, the original image is converted from the red green blue (RGB) colour space to YCbCrAQ1. The luminance signal Y is used to determine the frame type using histogram analysis. For HDR computation, frames are classified as dark, bright, and extreme types. Dark enhancement is applied to dark- and extreme-type frames to improve regions with low grey levels. On the other path, an inverse pattern y_{inv} is generated from an inverse kernel which includes 2×2 maximum fill, 3×3 low pass, and inverse operation. The inverted patterns y_{inv} are mixed using the factor of the original luminance signal. The results are then processed using brightness enhancement and automatic gain control (AGC) [14]. A colour HDR image is then generated via conversion from YCbCr to RGB.

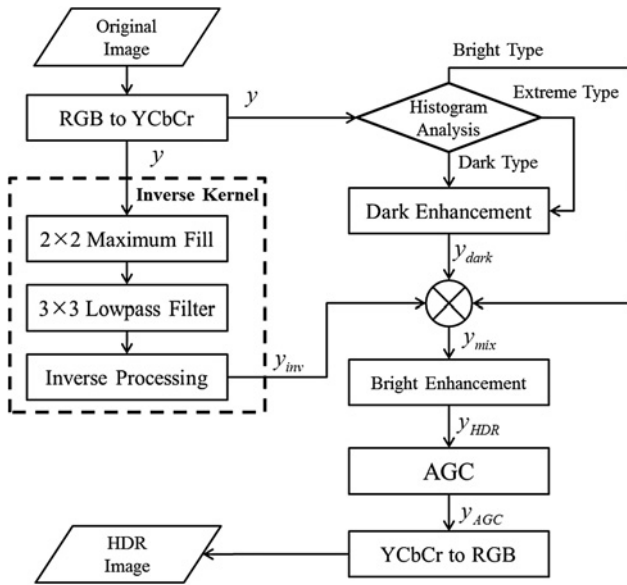


Fig. 1 Block diagram of the proposed HDR algorithm

2.1 Histogram analysis for type decision

When the current frame is sampled, we begin by estimating light distribution using histogram analysis before computing the HDR image. According to histogram distribution, the frame is classified into one of the following categories: (i) dark type, in which most of the image is of a low grey level, (ii) bright type, in which most of the image is of a high grey level, and (iii) extreme type, in which most of the image is of either a high or low grey level. To achieve this, we devised two parameters, H_i and L_o , for 8-bit images, which can be expressed as

$$\begin{cases} H_i = \sum_{i=Th3}^{Th4} h(i) + \sum_{i=Th4}^{255} h(i) \times 2 \\ L_o = \sum_{i=0}^{Th1} h(i) \times 2 + \sum_{i=Th1}^{Th2} h(i) \end{cases} \quad (1)$$

The symbol $h(i)$ represents the i th level of a histogram. Fig. 2 indicates the location of the histogram threshold. Parameter H_i indicates the portion of the image with a high grey level on the histogram between thresholds $Th3$ and $Th4$. To enhance the extra bright feature, the factor is multiplied by two between $Th4$ to 255 accumulating to H_i . Similarly, the parameter L_o represents to accumulate the double number of low-level range from 0 to $Th1$, and to accumulate the interval with the threshold from $Th1$ to $Th2$. $Th1 = 15$, $Th2 = 50$, $Th3 = 205$, and $Th4 = 240$ are used in experiments, where these values are not critical in practical applications. If the sampling image is too dark, then the L_o value will be large. Conversely, if the sampling image is too bright, then the H_i value will be large.



Fig. 2 Location of histogram threshold

Table 1 Condition of three types

Type	Condition
dark	$L_o > 2H_i$
bright	$H_i > 2L_o$
extreme	$\frac{1}{2} \leq (H_i/L_o) \leq 2$ and H_i and $L_o > (P_{total}/4)$
normal	other conditions

The frame type can be classified efficiently according to the parameters H_i and L_o , as shown in Table 1. If $L_o > 2H_i$, then the sample frame is of dark type. If $H_i > 2L_o$, then the sample frame is too bright; that is, bright type. Frames are classified as extreme type when $1/2 \leq (H_i/L_o) \leq 2$ and H_i and $L_o > (P_{total}/4)$, in which P_{total} is the number of total pixels, due to the fact that partial positive and negative saturation occurs in the same frame. Sampling frames that do not satisfy these conditions are deemed normal and do not require HDR processing. Figs. 3a–c present various types of sampling images and their corresponding histograms.

2.2 Inverse pattern generation kernel

The inverse kernel comprises three sub-modules: 2×2 maximum fill, a 3×3 low-pass filter, and an inverse operation. A detailed description of each block is listed as follows:

i. A 2×2 maximum fill is used to keep detail thin line information in Fig. 7 for HDR algorithm to overcome the distortion. Four pixels in a 2×2 block are filled using the maximum value of the four pixels, which can be expressed by

$$Y_{\max} = \max.(f_{i,j}, f_{i,j+1}, f_{i+1,j}, f_{i+1,j+1}). \quad (2)$$

$$\begin{bmatrix} f_{i,j} & f_{i,j+1} \\ f_{i+1,j} & f_{i+1,j+1} \end{bmatrix} = \begin{bmatrix} Y_{\max} & Y_{\max} \\ Y_{\max} & Y_{\max} \end{bmatrix}, \quad (3)$$

where the symbol $\max.$ is a maximum value search function. Y_{\max} is the maximum grey level at a 2×2 block. Figs. 4a and b present the original image and the result of 2×2 maximum fill.

ii. A 3×3 low-pass filter is used to smooth the pixels after 2×2 maximum filling operation, as follows:

$$y_{lpf}(i, j) = \frac{\sum_{k=-1}^1 \sum_{l=-1}^1 y_{\max}(i+k, j+l)}{9}, \quad (4)$$

where $y_{\max}(i, j)$ is the result of 2×2 maximum fill at coordinates (i, j) . The low-pass filter is used to smooth the jagged edges caused by the 2×2 maximum fill.

iii. An inverse operation achieves inverse function of input pixel in order to lighten dark areas and darken bright areas to avoid negative and positive saturation. We adopted a square linear function to improve performance in the dark regions. For an 8-bit image, this function is defined as follows:

$$y_{inv}(i, j) = \frac{(255 - y_{lpf}(i, j))^2}{255}. \quad (5)$$

The inverse function gives the maximum gain for the pixel with the lowest brightness. The gain gradually decreases with an increase in the grey value. Fig. 5 presents the transfer curve of (5) between input and output.

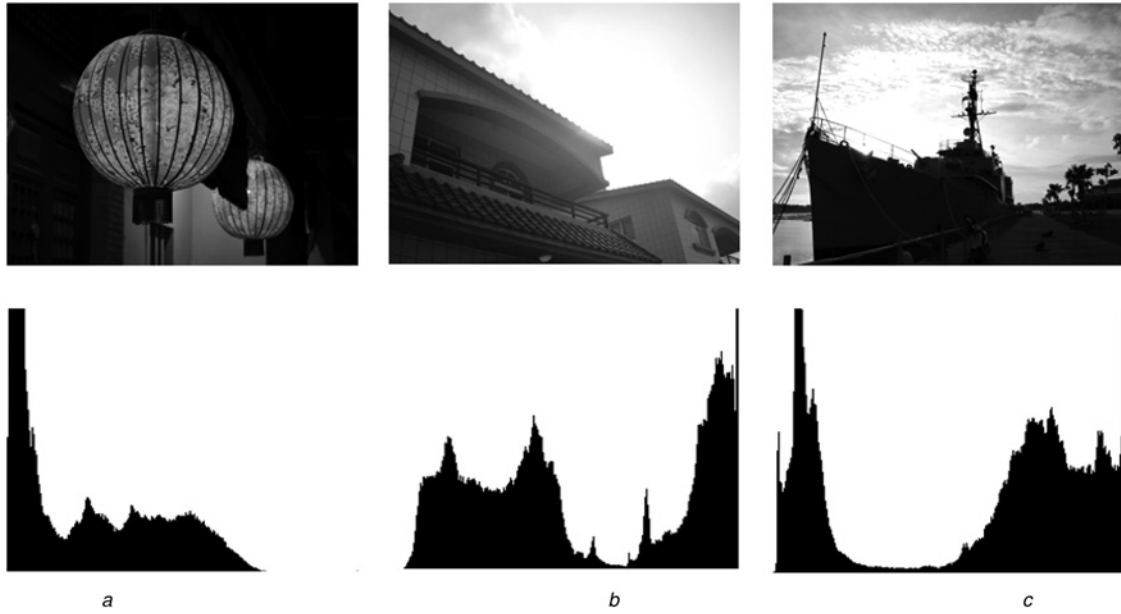


Fig. 3 Show the sampling picture and its histogram for

- a Dark type
- b Bright type
- c Extreme type

2.3 Mixing processing

To compensate for dim regions in dark-type and extreme-type frames, dark pixels are lightened as follows:

$$y_{\text{dark}}(i, j) = \begin{cases} y_{\text{in}}(i, j) + (\text{Th}_{\text{dark}} - y_{\text{in}}(i, j)) \times 0.05 & \text{if } y_{\text{in}}(i, j) < \text{Th}_{\text{dark}} \\ y_{\text{in}}(i, j) & \text{if } y_{\text{in}}(i, j) \geq \text{Th}_{\text{dark}} \end{cases} \quad (6)$$

where threshold Th_{dark} is defined by

$$\text{Th}_{\text{dark}} = \begin{cases} 128 & \text{if } y_{\text{in}} = \text{DarkType} \\ 50 & \text{if } y_{\text{in}} = \text{ExtremeType} \\ 0 & \text{if } y_{\text{in}} = \text{BrightType} \end{cases} \quad (7)$$

where y_{in} is the original input Y signal. This operation includes a minimum value for pixels of a low grey level in order to avoid negative saturation. If y_{in} is low, the grey level is increased using (6). When the frame type is dark, the grey level is enhanced for all pixels scoring < 128 . For extreme-type frames, the brightness of the pixels is increased only if the grey level is < 50 . For bright frames, that is, when $\text{Th}_{\text{dark}} = 0$, no brightening is performed.

Similar to LCD local-dimming backlight theory [13], y_{dark} is an original low dynamic range image and y_{inv} is used in a manner similar to that of a backlight signal. We perform a mixing operation of the inverse pixel from (5) and enhanced pixel from

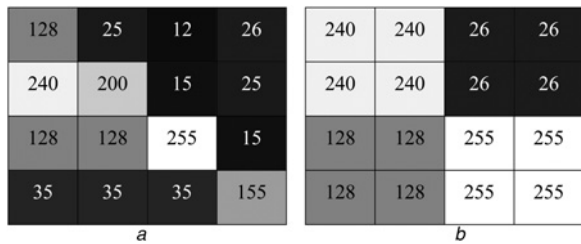


Fig. 4 Inverse pattern generation kernel of

- a Original image
- b Results with 2×2 maximum fill

(6) using the following equation:

$$y_{\text{mix}}(i, j) = y_{\text{dark}}(i, j) \times y_{\text{inv}}(i, j) \times k \quad (8)$$

where k is a key parameter identifying the HDR image. Parameter k is an adaptive value that depends on features in the sample image. The maximum value of $y_{\text{mix}}(i, j)$ is limited at 255, for an 8-bit grey image. Increasing the value of k results in a more pronounced HDR effect. The dark portion is made brighter because the value of its inverse backlight y_{inv} is high. In the opposite case, the bright pixels are made darker due to low y_{inv} to prevent pixels from becoming over-exposed. We selected the three images shown in Fig. 6 for testing. A high value for Lo implies that there are many dark pixels in the frame, which necessitates a larger k for the adjustment of brightness.

Next, we devised an adaptive k parameter to process any type of frame. To find the linearly proportional relationship between k and Lo , we use the following equation:

$$k - k_1 = \frac{k_2 - k_1}{\text{Lo}_2 - \text{Lo}_1} \times (\text{Lo} - \text{Lo}_1), \quad (9)$$

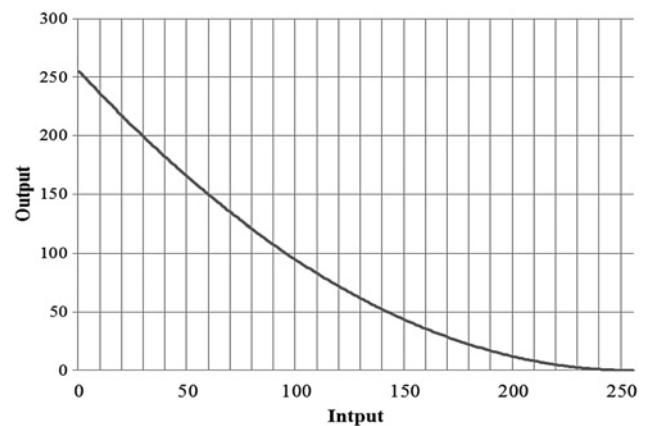


Fig. 5 Conversion curve of inverse processing

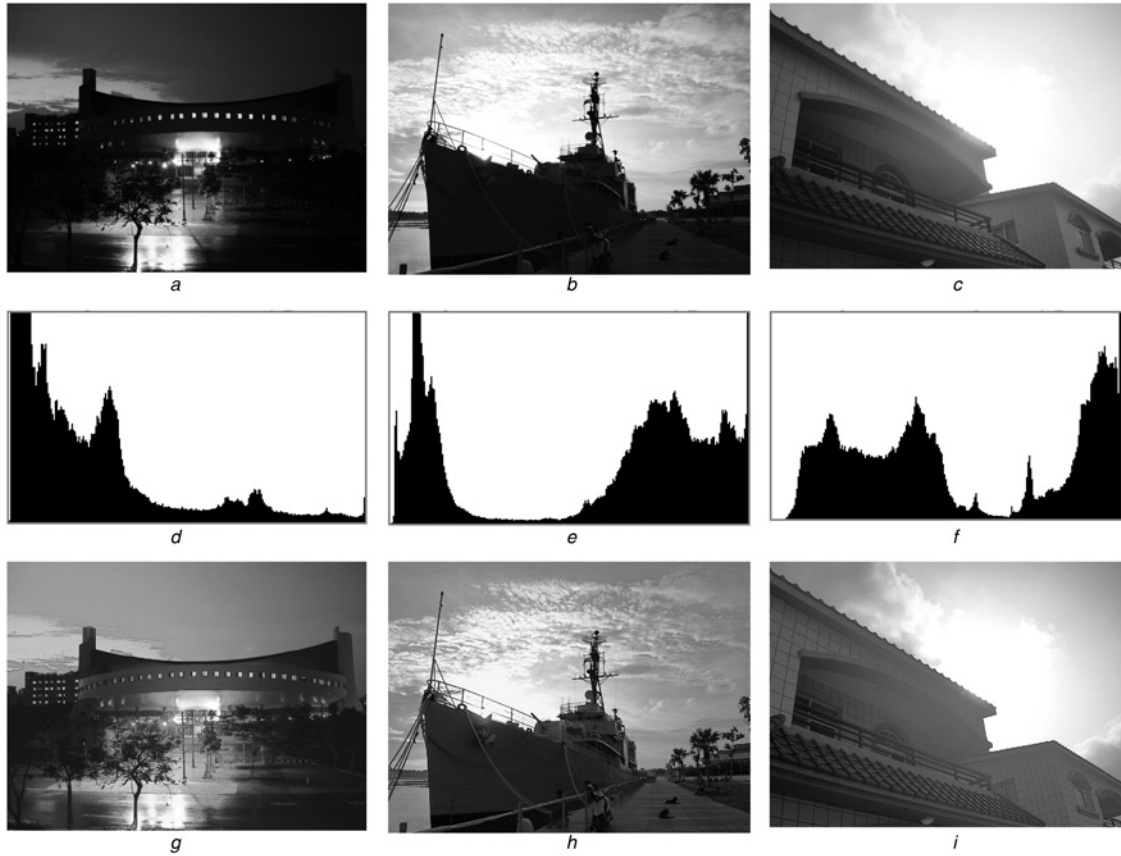


Fig. 6 Three original images

- a* Dark type
- b* Extreme type
- c* Bright type
- d* Histogram of dark type, $Lo = 483,971$
- e* Histogram of extreme type, $Lo = 193,245$
- f* Histogram of bright type, $Lo = 75,469$
- g* HDR results of dark type with difference k , $k = 0.0178$
- h* HDR results of extreme type with difference k , $k = 0.0125$
- i* HDR results of bright type with difference k , $k = 0.0104$

where $[(k_2 - k_1)/(Lo_2 - Lo_1)]$ denotes the linear slope. When the slope is small, the linear variation is reduced. According to the results in Fig. 6, we can attain the slope using

$$m = \tan \theta = \frac{k_2 - k_1}{Lo_2 - Lo_1} = \frac{0.0178 - 0.0125}{483,971 - 193,245} \cong 1.82 \times 10^{-8}. \quad (10)$$

When the sampling image is dark, the estimated Lo value is large; therefore, the parameter k is increased to improve brightness.

Thus, k is determined according to the corresponding Lo value. To determine k for a given Lo value, we use a standard linear equation as follows:

$$k = m \times Lo + b, \quad (11)$$

where b is an offset. Thus, (9) can be rewritten as follows:

$$k = m \times Lo - m \times Lo_1 + k_1. \quad (12)$$

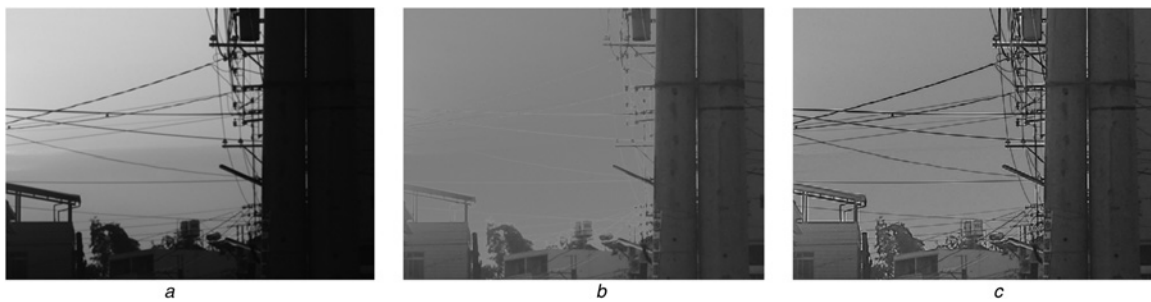


Fig. 7 Simulations and comparisons of

- a* Original image
- b* HDR processing without 2×2 maximum fill
- c* HDR processing with 2×2 maximum fill

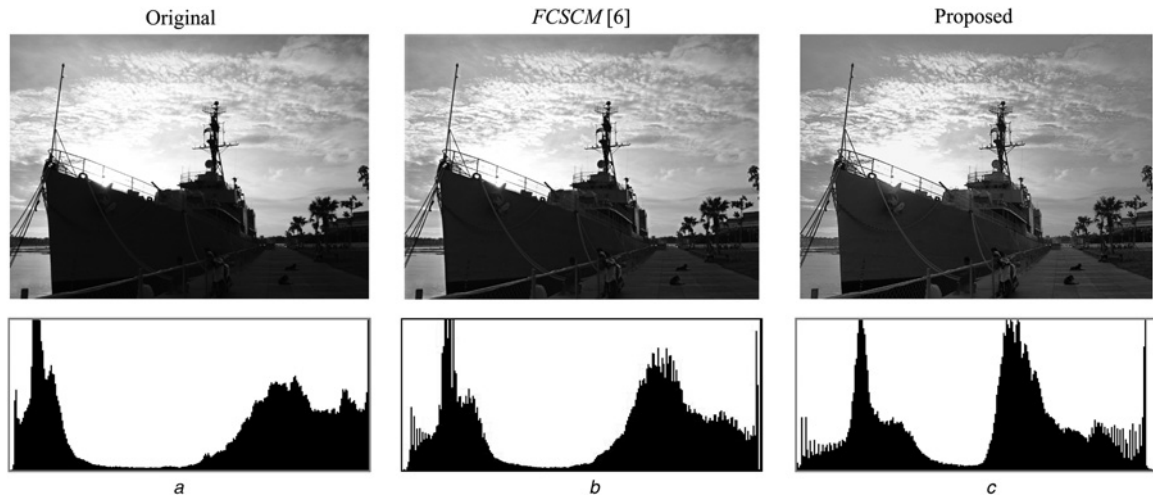


Fig. 8 Original image, and the result of [6] and the proposed method for extreme type

a HB = 384,180
b HB = 343,110
c HB = 317,534, $k = 0.0125$

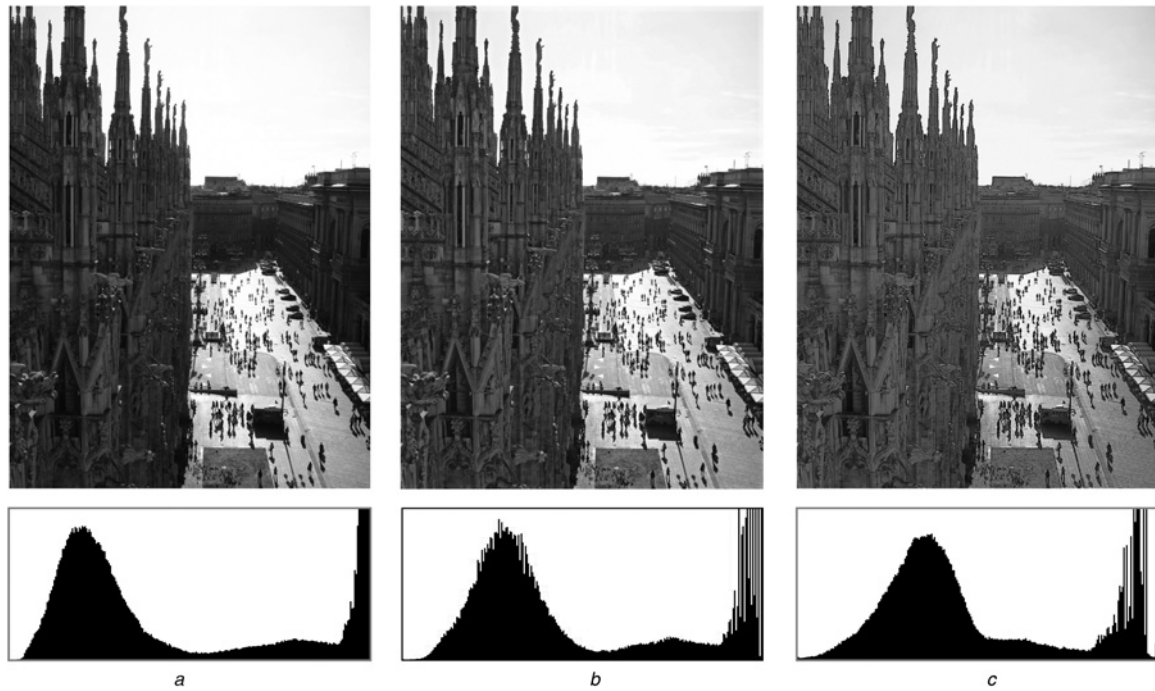


Fig. 9 Original image, and the result of [6] and the proposed method for extreme type

a HB = 442,248
b HB = 418,368
c HB = 394,906, $k = 0.0113$

Offset value b can be computed using (11) and the parameters (Lo ; k), which can be found in Figs. 6*e* and *h*. The result of offset b is close when using other points. The linear relationship of b , k , and Lo can therefore be expressed using the following equation:

$$b = k_1 - m \times Lo_1 = 0.0125 - 1.82 \times 10^{-8} \times 193,245 \cong 0.009. \quad (13)$$

Finally, the linear relationship between k and Lo can therefore be expressed by

$$k = 1.82 \times 10^{-8} \times Lo + 0.009. \quad (14)$$

After the mixing operation, the luminance of the dark region is increased and the bright region is compressed. To expand the dynamic range, the grey level is increased using the following operation: (see (15))

If y_{dark} from (6) is larger than the threshold Th_b , the grey level is increased using (15). Experiment results lead us to select $Th_b = 50$.

Generally, halos occur between the foreground and over-exposed regions of the background, as shown in Fig. 3*b*. The proposed method can suppress halos by increasing darkness levels and decreasing brightness levels. Finally, we expand the luminance range from 0 to 255 using AGC and enhance the colour using RGB pixels processing [14].

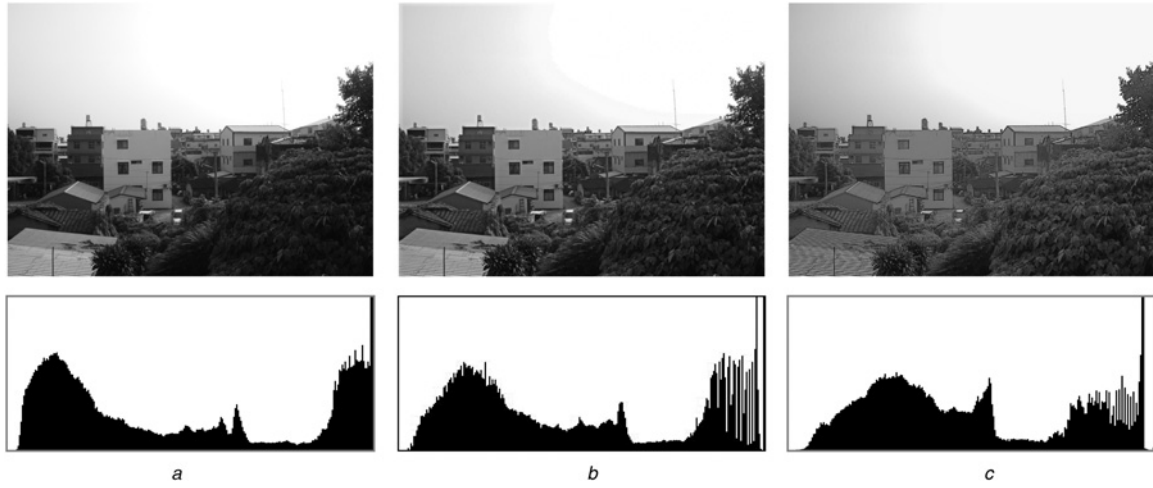


Fig. 10 Original image, and the result of [6] and the proposed method for extreme type

a HB = 409,432
b HB = 360,508
c HB = 307,974, $k = 0.0117$

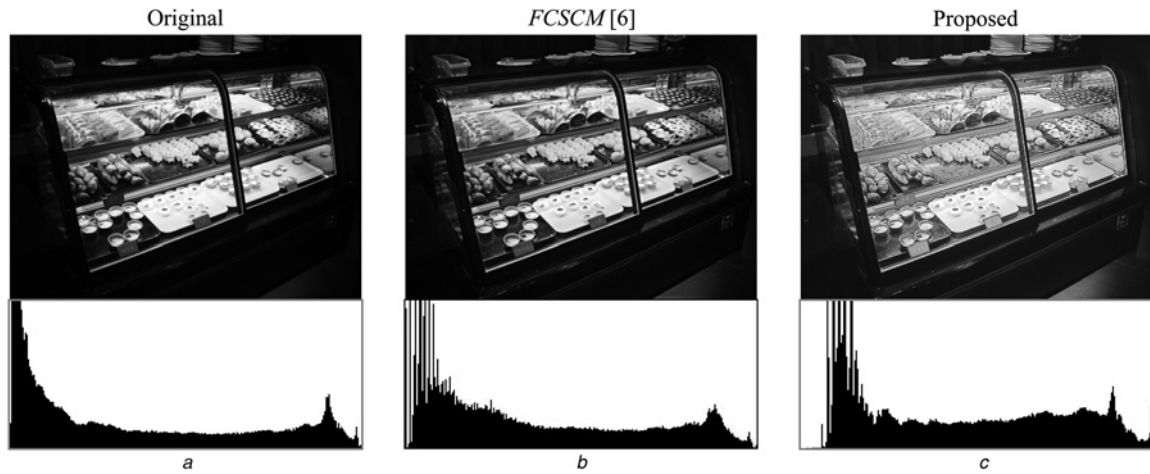


Fig. 11 Original image, and the result of [6] and the proposed method for dark type

a HB = 475,654
b HB = 407,864
c HB = 353,938, $k = 0.0195$

3 Simulations and comparisons

We sampled various types of images to evaluate the proposed HDR method. First, we estimate with and without using maximum fill in the inverse kernel. Fig. 7a shows the original image, which contains many thin dark lines. When a dark line is very thin (< 3 pixels), the grey level of the pixels in the line is low, even after 3×3 low-pass processing except in the case where 2×2 maximum fill is used. The grey level is then increased using the inverse processing in (5). The luminance values of the thin dark lines are increased through application of the mixing processing presented in (8). This causes the lines to disappear by reducing the difference between the line and background, as shown in Fig. 7b. To overcome this difficulty, we first used 2×2 maximum fill to enable the 3×3 low-pass filter to cover more white background pixels. Thus, the grey level of pixels is increased after 3×3

low-pass processing. The grey level decreases after the inverse processing. The thin dark lines will be relatively too low after mixing processing, which has obvious contrast to white background. These thin lines are retained after HDR processing, as shown in Fig. 7c. This demonstrates that a 2×2 maximum fill operation is required for our proposed algorithm to maintain information related to fine details.

To estimate the performance of the HDR algorithm using subjective assessment, we defined a parameter related to the histogram balance (HB) as follows:

$$HB = \sum_{i=0}^{255} \left| h(i) - \frac{\text{height} \times \text{width}}{256} \right|, \quad (16)$$

where $\text{height} \times \text{width}$ refers to the size of the frame. The image

$$y_{\text{HDR}}(i, j) = \begin{cases} y_{\text{mix}}(i, j) + (y_{\text{dark}}(i, j) - Th_b)^2 \times 0.005 & \text{if } y_{\text{dark}}(i, j) \geq Th_b \\ y_{\text{mix}}(i, j) & \text{if } y_{\text{dark}}(i, j) < Th_b \end{cases} \quad (15)$$

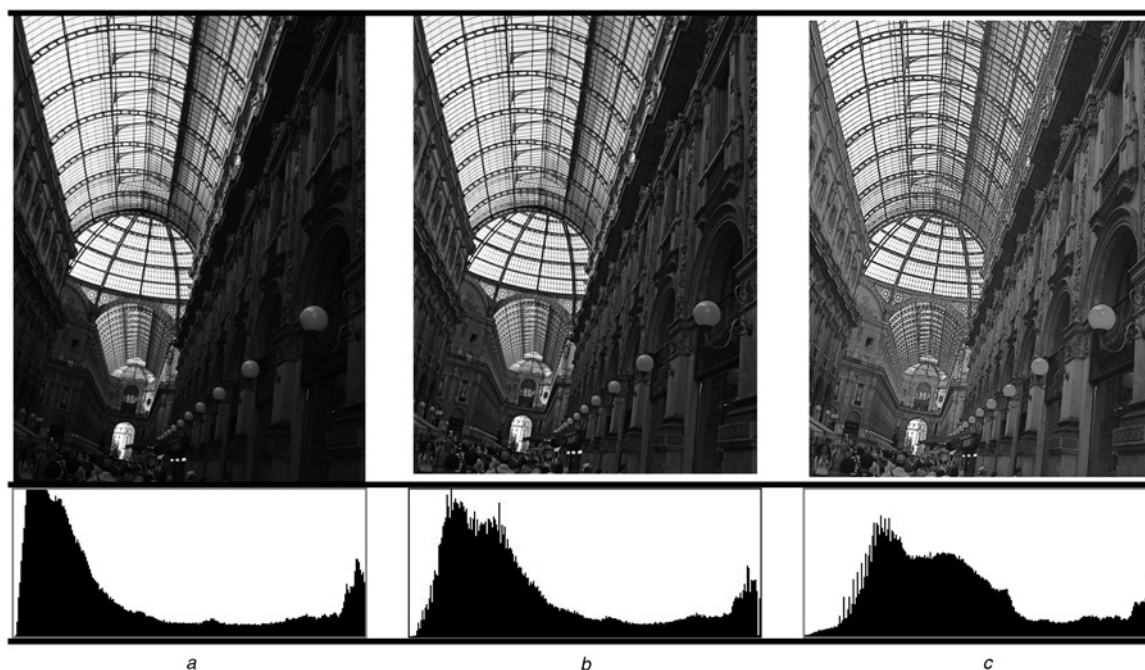


Fig. 12 Original image, and the result of [6] and the proposed method for dark type

a HB = 398,796

b HB = 343,832

c HB = 309,780, $k = 0.0153$

resolution is 8 bits; therefore, the number of grey levels is 256. Thus, the average histogram level is given by $(\text{height} \times \text{width})/256$. When each $h(i)$ is close to the histogram average, HB is reduced, indicating that the distribution of the grey levels is relatively uniform. Thus, the dynamic range of the image is expanded.

For comparisons, we selected one HDR algorithm based on fast centre-surround contrast modification (FCSCM) [6] using one time exposure to process a single frame. This algorithm can solve the problem of under- and over-exposed sampling. The sample images were processed using FCSCM and the proposed algorithm, respectively, before undergoing objective as well as subjective evaluation.

We selected sampling images representative of extreme-, dark-, and bright-type frames. Figs. 8 to 10a–c present extreme-type frames, in which many pixels that are near negative and positive saturation locate on low and high levels at the same frame.

FCSCM [6] was able to reduce the HB value and improve the image quality. The proposed algorithm adaptively computed the k value to suit various images for HDR image generation. Our results show that the proposed algorithm achieved a lower HB resulting in superior image quality, compared with the results in [6]. The results of processing dark-type images are presented in Figs. 11 to 13a–c. For dark-type images, the k value is adaptively increased to brighten dim regions. Finally, we tested bright-type images, which may contain positive saturation pixels. According to our algorithm, for this type of image, k must be small. The grey level of pixels in overly bright regions can be reduced to avoid positive saturation, as shown in Figs. 14 and 15a–c. Clearly, the positive saturation pixel can be reduced in histogram distribution. According to these results, the proposed method indeed improves the image quality when viewed objectively and provides a better HB value in subjective analysis.



Fig. 13 Original image, and the result of [6] and the proposed method for dark type

a HB = 479,788

b HB = 378,626

c HB = 323,734, $k = 0.0187$

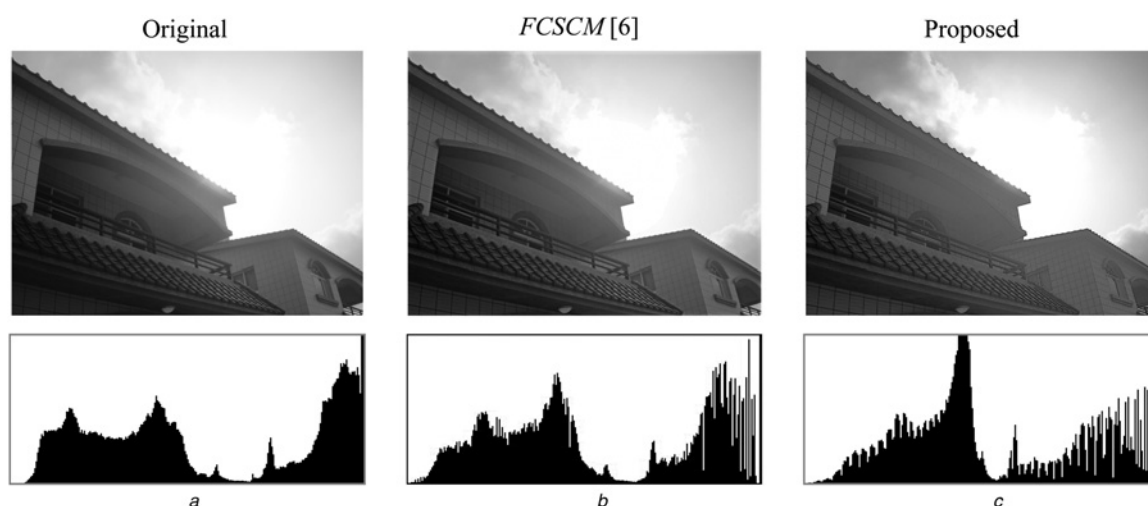


Fig. 14 Original image, and the result of [6] and the proposed method for bright type

a HB = 315,822
b HB = 318,028
c HB = 339,708, $k = 0.0104$

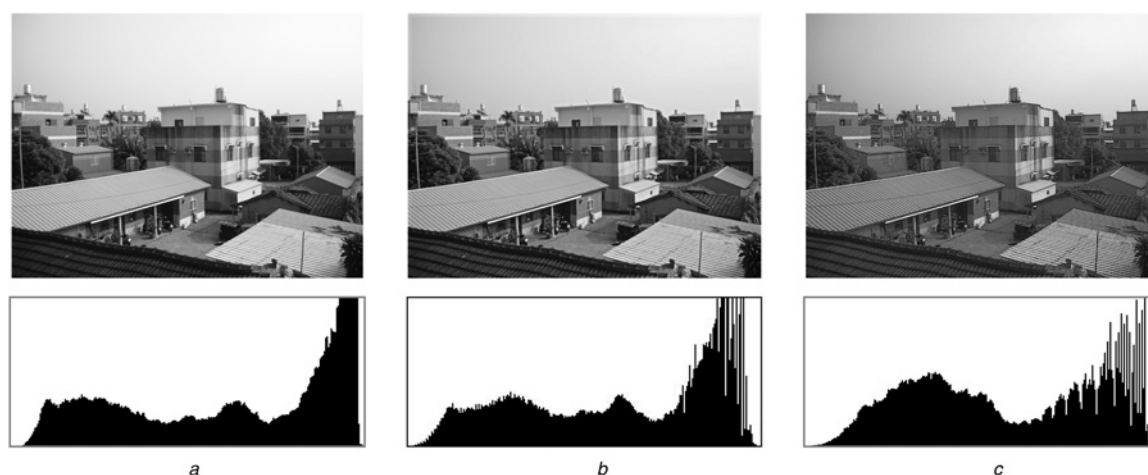


Fig. 15 Original image, and the result of [6] and the proposed method for bright type

a HB = 247,890
b HB = 241,132
c HB = 227,234, $k = 0.0101$

The results of objective evaluation are outlined in Table 2, which lists the HB value of all test images including the originals, and the results obtained using the method in [6], as well as the proposed method. The proposed method reduced the HB value by an average of 18%, compared with the original image, which is an improvement of 8% greater than that of the competing algorithm [6]. Clearly, the proposed HDR algorithm achieves superior performance in both objective as well as subjective evaluation.

The computation of the proposed method includes histogram analysis for type decision, inverse pattern generation kernel, and mixing processing. The first used two accumulators to accumulate the number of low-level and high-level histograms. The second used simple fill operation, low-pass filter, and inverse curve mapping. The last used linear equations to find adaptive parameter and then to calculate HDR image. The computation complexity is an $O(N)$ (N is the number of image pixels), which is closed to the competing algorithm [6] and better than [2, 4, 7].

Table 2 Average HB of Figs. 8–15 using difference methods

Images	Type	Original	FCSCM [6]	Proposed
Fig. 8	extreme	384,180	343,110	317,534
Fig. 9	extreme	442,248	418,368	394,906
Fig. 10	extreme	409,432	360,508	307,974
Fig. 11	dark	475,654	407,864	353,938
Fig. 12	dark	398,796	343,832	309,780
Fig. 13	dark	479,788	378,626	323,734
Fig. 14	bright	315,822	318,028	339,708
Fig. 15	bright	247,890	241,132	227,234
average HB		394,226	351,434	321,851

4 Conclusions

This paper presents a high-performance HDR algorithm which can be implemented using a single frame. Based on the principle of LCD backlighting, an inverse pattern is adaptively generated according to the imaging data. Through the use of frame-type classification, the HDR algorithm is able to adaptively compute parameters to suit a variety of image features. Results demonstrate that the proposed algorithm is able to produce high-quality HDR images by adjusting under-exposed as well as over-exposed

regions. The resulting HDR images appear natural, rather than artificial. The proposed algorithm uses single-pass processing instead recursive processing, which helps to reduce computational costs, making it suitable for processing in real time. For subjective measurement, we developed the HB parameter to evaluate the performance of HDR algorithm. Compared with the original image and the results of an existing HDR method [6], the proposed algorithm improved the HB value by 18 and 8%, respectively. High-performance and rapid computational capability make the proposed algorithm applicable to real-time camera imaging systems.

5 Acknowledgments

This work was supported by the Acard Technology Corp. and the National Science Council, Taiwan, under NSC 100-2221-E-224-059-MY3.

6 References

- 1 Mann, S.: 'Compositing multiple pictures of the same scene'. Proc. of the 46th Annual IS&T Conf., Cambridge, MA, 1993, pp. 50–52
- 2 Robertson, M.A., Borman, S., Stevenson, R.L.: 'Estimation-theoretic approach to dynamic range enhancement using multiple exposures', *J. Electron. Imaging*, 2003, **2**, (12), pp. 219–228
- 3 Ramachandra, V., Zwicker, M., Nguyen, T.: 'HDR imaging from differently exposed multiview videos'. Proc. IEEE 3DTV-CON'08, Istanbul, Turkey, 2008, pp. 85–88
- 4 Várkonyi-Kóczy, A.R., Rövid, A., Hashimoto, T.: 'Gradient-based synthesized multiple exposure time color HDR image', *IEEE Trans. Instrum. Meas.*, 2008, **57**, (8), pp. 1779–1785
- 5 Vavilin, A., Jo, K.H.: 'Fast HDR image generation from multi-exposed multiple-view LDR images'. Proc. IEEE Int. Conf. on European Workshop on Visual Information Processing, 2011, pp. 105–110
- 6 Vonikakis, V., Andreadis, I., Gasteratos, A.: 'Fast centre-surround contrast modification', *IET Image Process.*, 2008, **2**, (1), pp. 19–34
- 7 Guarnieri, G., Marsi, S., Ramponi, G.: 'High dynamic range image display with halo and clipping prevention', *IEEE Trans. Image Process.*, 2011, **20**, (5), pp. 1351–1362
- 8 Kim, K., Bae, J.n., Kim, J.: 'Natural HDR image tone mapping based on retinex', *IEEE Trans. Consum. Electron.*, 2011, **57**, (4), pp. 1807–1814
- 9 Mann, S., Ovtcharov, R.C.H., Lo, K., *et al.*: 'Realtime HDR (high dynamic range) video for eyetap wearable computers, FPGA-based seeing aids, and glasseyes (eyetaps)'. Proc. IEEE Int. Conf. on 25th IEEE Canadian Conf. on Electrical and Computer Engineering (CCECE), 2012, pp. 1–6
- 10 Zhao, Jin, Shen J.: 'Real-time tone mapping for high-resolution HDR images'. Proc. IEEE Int. Conf. on Cyberworlds, 2008, pp. 256–262
- 11 Lee, J.S., Chen, C.H., Chang, C.C.: 'A novel illumination-balance technique for improving the quality of degraded text-photo images', *IEEE Trans. Circuits Syst. Video Technol.*, 2009, **19**, (6), pp. 900–905
- 12 Kim, J.Y., Kim, L.S., Hwang, S.H.: 'An advanced contrast enhancement using partially overlapped sub-block histogram equalization', *IEEE Trans. Circuits Syst. Video Technol.*, 2001, **11**, (4), pp. 475–484
- 13 Hsia, S.C., Sheu, M.H., Chien, J.R.C., Wang, S.K.: 'High-performance local dimming algorithm and its hardware implementation for LCD backlight', *IEEE J. Disp. Technol.*, 2013, **9**, (7), pp. 527–535
- 14 Hsia, S.C., Tsai, P.S.: 'Low-complexity camera digital signal imaging for video document projection system', *SPIE J. Electron. Imaging*, 2011, **20**, (2), pp. 1–10